

TOPFLOW TESTS ON THE STRUCTURE OF THE GAS-LIQUID INTERFACE IN A LARGE VERTICAL PIPE

Horst-Michael Prasser, Matthias Beyer, Arnd Boettger, Helmar Carl, Dirk Lucas, Andreas Schaffrath, Peter Schuetz, Frank-Peter Weiss, and Jochen Zschau

1. Introduction

TOPFLOW is an acronym deduced from Transient Two Phase FLOW Test Facility [1, 2]. It is designed for generic and applied studies of transient two phase flow phenomena in power and process industries. The fluid is either steam-water or air-water mixture. TOPFLOW stands in the tradition of single-effect tests in large-scale models of safety relevant components of nuclear plants. The new test facility in Rossendorf was constructed using parts of NOKO, a test facility, which was successfully operated at the Forschungszentrum Jülich [3]. NOKO was dismantled in 2001, the electrical heater and the condenser tank were transferred to the new site in Rossendorf and completed by a number of new components. In the end of 2002 the facility was commissioned and reached its working parameters of 7 MPa and the corresponding saturation temperature of 286 °C.

After this, first tests were carried out that aimed at studying the structure of a gas-liquid two-phase flow in pipes of large diameter. For this purpose, an air-water flow in the large vertical test section of TOPFLOW was studied using a wire-mesh sensor [4, 5]. Its high spatial and temporal resolution allow to obtain time sequences of instantaneous gas fraction distributions over the entire cross section that reflect the shape and extension of the gas-liquid interface in great detail. The data is used for the visualisation of the two-phase flow structure as well as to obtain void fraction profiles and bubble size distributions [6, 7]. Additionally to earlier described methods, a new visualisation technique is presented, that consists in the creation of virtual side projections of the flow. Using these three evaluation methods, new insights are brought into the structure of two-phase flow in large pipes. The comparison with earlier tests in a 51.2 mm pipe revealed scaling effects.

2. Test section DN 200

The test pipe has an inner diameter is 194.1 mm and a total height of 9 m. Close to the lower end a gas injector is located (Fig. 1). A tube is bend into the main flow direction, forming a coaxial segment which has a perforated head to inject the air. The perforation consists of three rings, each with 20 orifices of 6 mm diameter (Fig. 2). Above the perforated region the injector head has a conical part in order to reduce the formation of vortices due to flow separation effects.

The new wire-mesh sensor (Fig. 3) comprises a matrix of 64x64 measuring points that are scanned at 2500 Hz. The large number of electrode wires allows to achieve a resolution of 3 mm in the entire cross section. The sensor is mounted into a flange connection 1000 mm below the upper end of the test section. The distance between gas injection and the measuring plane of the wire-mesh sensor was $z_{\text{wms}} = 7660$ mm.

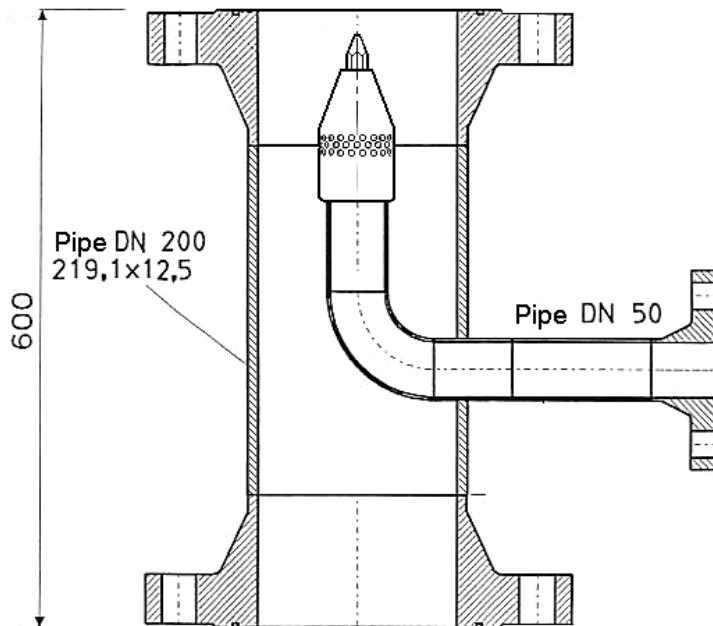


Fig. 1: Gas injection device in the DN200 test pipe

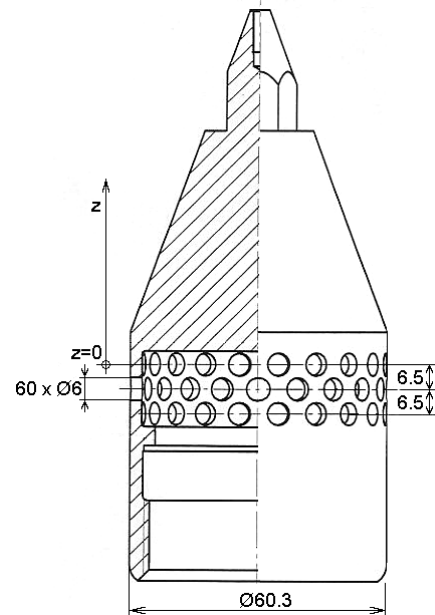


Fig. 2: Gas injection head

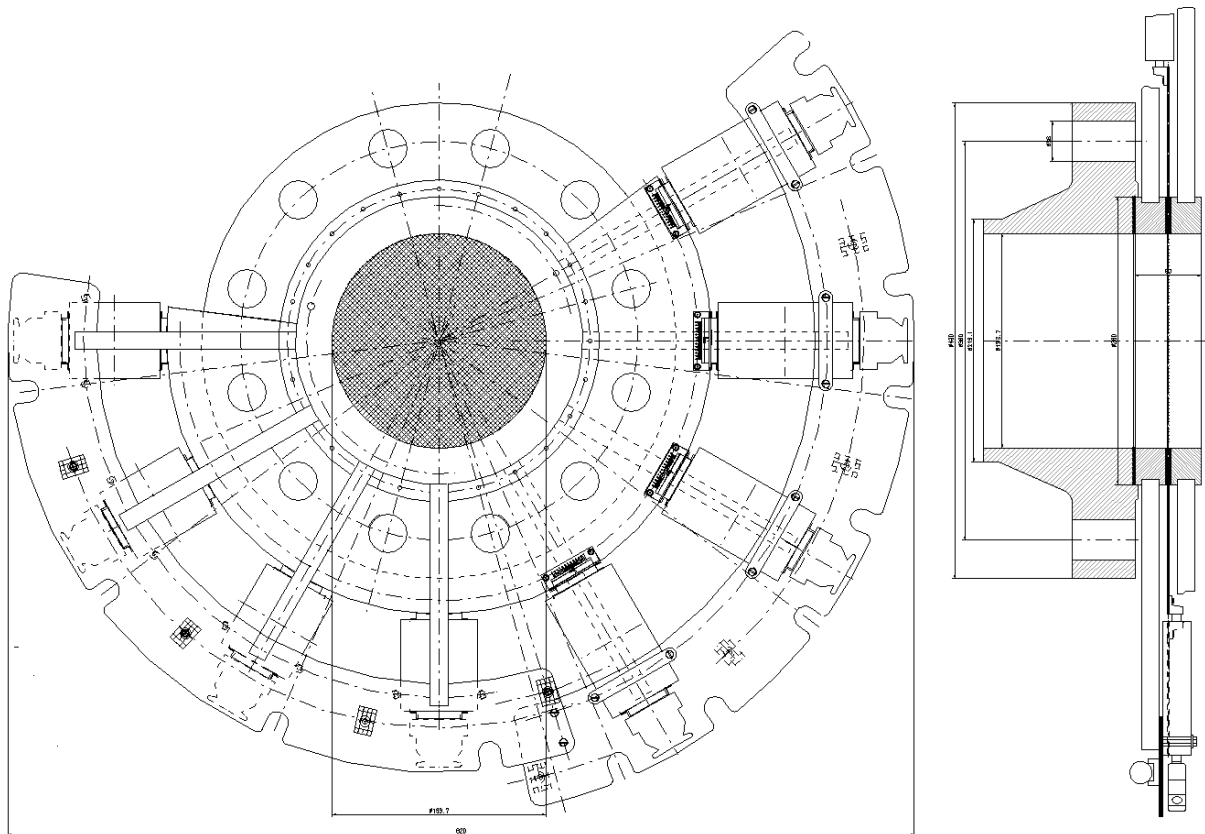


Fig. 3: Wire-mesh sensor for the DN200 test pipe with a measuring matrix of 64x64 points

3. Methods of wire-mesh sensor data visualisation

Conductivity distributions measured by the wire-mesh sensor are transformed into sequences of instantaneous two-dimensional gas fraction distributions by relating the conductivity of the gas-liquid mixture to the conductivity of plain liquid. After this operation (a tomographic image reconstruction is not necessary) the gas fraction distribution can be used for visualisation purposes.

The construction of virtual sectional views is a powerful method [7]: distributions over the pipe diameter are plotted as horizontal bars and a time sequence of such bars is arranged in a vertical order starting from the top of the image. In the result, the plot obtains the character of a sectional view onto the flow structure at a vertical plane situated in the centre of the pipe. The vertical axis is transformed into a virtual z-axis by scaling it according to the velocity of the gaseous phase. If the lateral axis is kept in the same scale as this virtual z-axis, bubbles are displayed without distortion, i.e. with the right length-to-width relation. Since individual bubble velocities are not available, the average phase velocity calculated from the known superficial gas velocity divided by the measured average gas fraction is used as an approximation. This leads to a certain distortion, since the velocity differs from bubble to bubble and shows a characteristic profile with a maximum in the centre of the pipe. The scaling according to the average velocity is nevertheless a helpful procedure to obtain an approximate visualization of the real shape of the bubbles. It is a big advantage of the virtual z-axis, that sectional plots obtained at different air flow rates can be directly compared.

Since virtual sectional views do not show bubbles moving in front or behind the chosen sectional plane, it is useful to complement this method by virtual side projections [5]. They represent the entire information from the measuring cross-section, which is transformed into a virtual side view using a simplified ray-tracing algorithm. To perform this kind of imaging, it is assumed that parallel white light propagates through a three-dimensional column containing the measured gas fraction distribution. The light arriving from aside is partially absorbed and partially scattered towards the observer in front of the column. A simulated image seen by the observer is calculated under the assumption of different absorption and scattering coefficients for each colour component of the light, i.e. a set of individual coefficients for red, green and blue is defined empirically to obtain high contrast between the phases and a plastic impression. Length and width of the image are again scaled considering the average gas velocity. As a result, a life-like image of the flow pattern is created, which is close to the view through a transparent pipe wall.

4. Results

As a result of scaling studies, Ohnuki [8] reported, that the slug flow found in small pipes does not occur in larger pipes (diameters 200 mm and 480 mm). The authors compared their results with those of Leung [9] performed at $D = 25.4$ mm and Liu et al. [10] at $D = 38$ mm as well as with the flow maps of Serizawa and Kataoka [11]. Visual observations revealed that in the large pipes an immediate transition from bubbly to churn turbulent flow was found instead of a slug flow. Typical Taylor bubbles that occupy almost the entire cross section occur only in small pipelines. It was assumed that the boundary condition at the pipe walls stabilise the Taylor bubbles in the small pipes.

The plots obtained with the method of virtual side projections confirm the visual observations of Ohnuki [8] (Fig. 4). Large bubbles appear in the flow, the size of which grows rapidly with increasing superficial gas velocity. In the same time, the flow takes a more and more irregular structure, bubble density becomes very inhomogeneous. At high gas flows, the flow pattern becomes churn turbulent, i.e. regular structures disappear completely. Finally, large bubbles are hardly visible anymore since the view is obstructed by the irregular swarms of small bubbles. This gives reason to the conclusion that a transition to churn turbulent flow has taken place.

Virtual sectional side views allow a look into the mid-plane of the pipe without the increasing obstruction of the view by bubbles close to the pipe wall. Such plots reveal that large bubbles are still present, their size and number increases with growing air flow rate (Fig. 5).

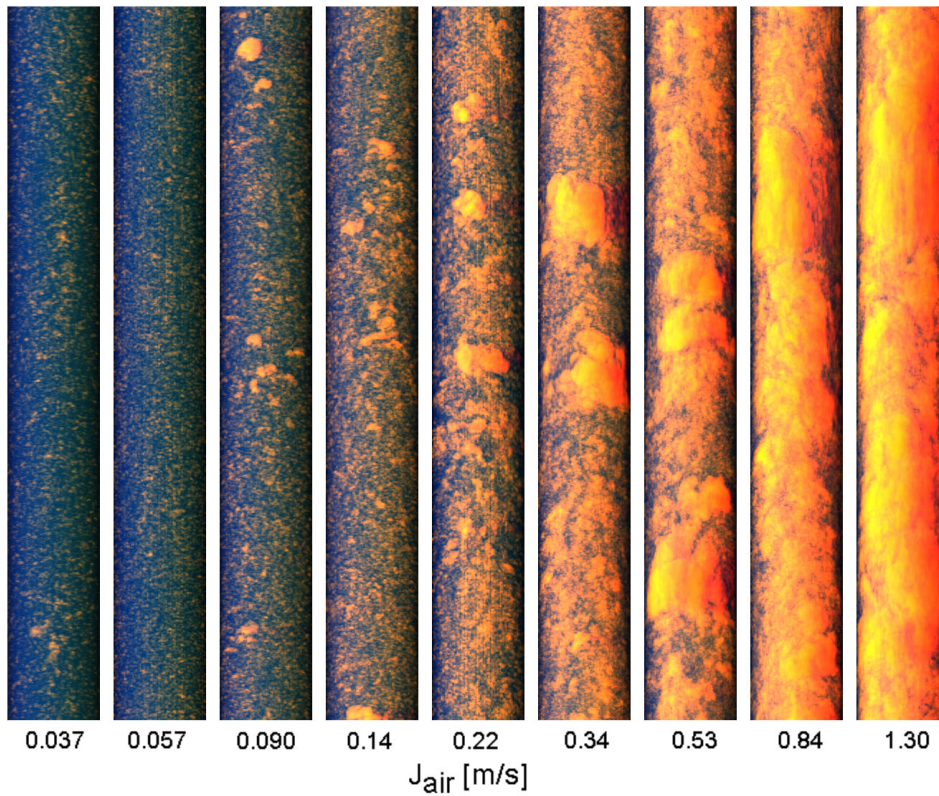


Fig. 4: Virtual side projections of the gas distribution in the DN200 test section, $J_{\text{water}} = 1 \text{ m/s}$, ratio of vertical to horizontal scale = 1:1, height scaled according to average gas velocity, gas - red to yellow, liquid - blue

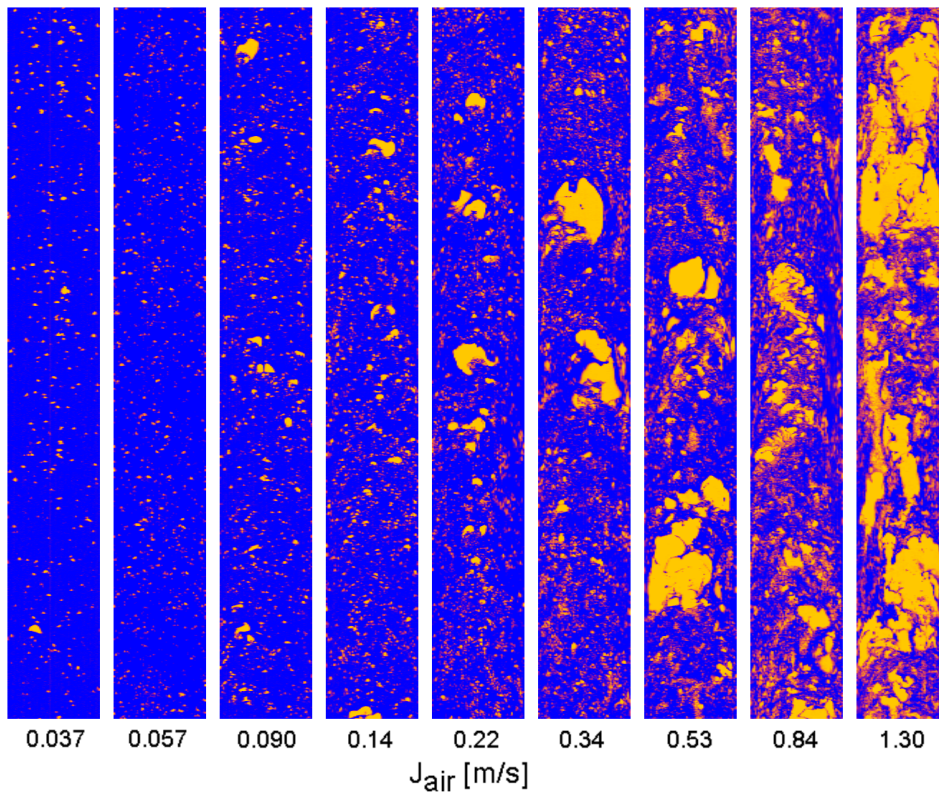


Fig. 5: Virtual sectional views of the void distribution in the DN200 test section, $J_{\text{water}} = 1 \text{ m/s}$, scaling see Fig. 4, yellow - gas, blue - liquid

Bubble size distributions show the appearance of a bimodal distribution at a superficial gas velocity of about 0.14 m/s. They confirm the observations in Fig. 5, since a further increase of the gas flow leads to a continuous growth of the large-bubble peak in the distribution. The appearing second peak is shifted towards higher diameters, it becomes wider and the amplitude increases.

A direct comparison between bubble size distributions obtained in the two different pipes revealed that the second peak appears at lower superficial gas velocities in the pipe DN50. At a superficial gas velocity that corresponds to the slug flow region in the DN50 pipe the large bubble fraction shows equivalent diameters which are greater than the pipe diameter (see [12]), i.e. the peak is caused by large elongated Taylor bubbles. In the DN200 pipe a bimodal bubble size distribution was found, too (Fig. 6). The bubbles of the large fraction are much larger than in the small pipe, while their contribution to the overall gas fraction (peak height) is smaller. On the other hand, the peaks are much broader.

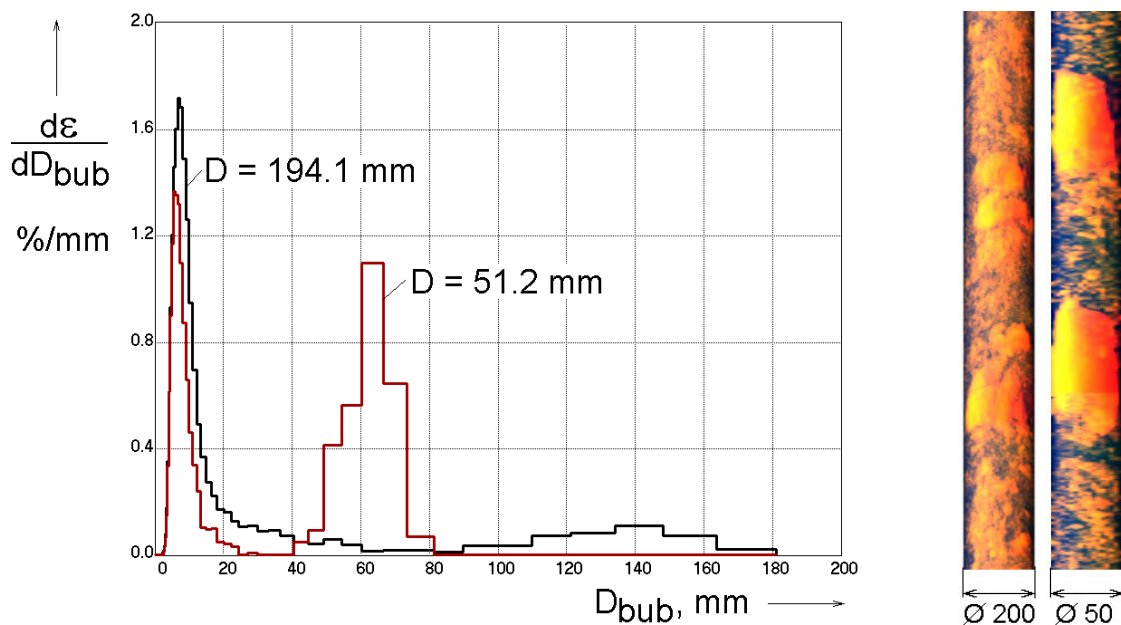


Fig. 6: Comparison of bubble size distributions in DN50 and DN200 test sections for an air flow rate typical for slug flow in pipes of small diameter, superficial velocities: $J_{\text{air}} = 0.53 \text{ m/s}$, $J_{\text{water}} = 1 \text{ m/s}$

In the large pipe, big bubbles can move much more freely, which leads to a higher probability of collisions between them than in the small pipe, where the separating liquid slug has to be drained off, before two Taylor bubbles can coalesce. This hypothesis would explain the observed larger bubble sizes in the bigger pipe.

Additionally to the calculation of bubble size distributions, the bubble identification procedure [6] can be applied to extract individual bubbles from the data array and display them individually. For this purpose the local instantaneous gas fractions in all elements not belonging to the selected bubble are put to zero. When the resulting new distribution is displayed by one of the mentioned visualization techniques, the selected bubble becomes visible without all the other surrounding bubbles, which otherwise may have obstructed the view. In turn it is also possible to eliminate a selected bubble and the display only the surrounding bubbles. For this, the gas fractions of elements labelled by the number of the given bubble have to be set to zero.

This method was applied to extract several large bubbles found in the wire-mesh data at high superficial gas velocities. In Fig. 7 virtual side projections constructed in this way are shown. In the left column, the original data is displayed, the column in the centre presents the virtual projection view of the selected bubble and, finally, the right column shows the flow structure remaining after eliminating the large bubble. It is clearly visible, that the large bubble is heavily deformed as a result of the action of turbulence to the gas-liquid interface. At the given high air flow rate, the bubble was found to be about 660 mm tall.

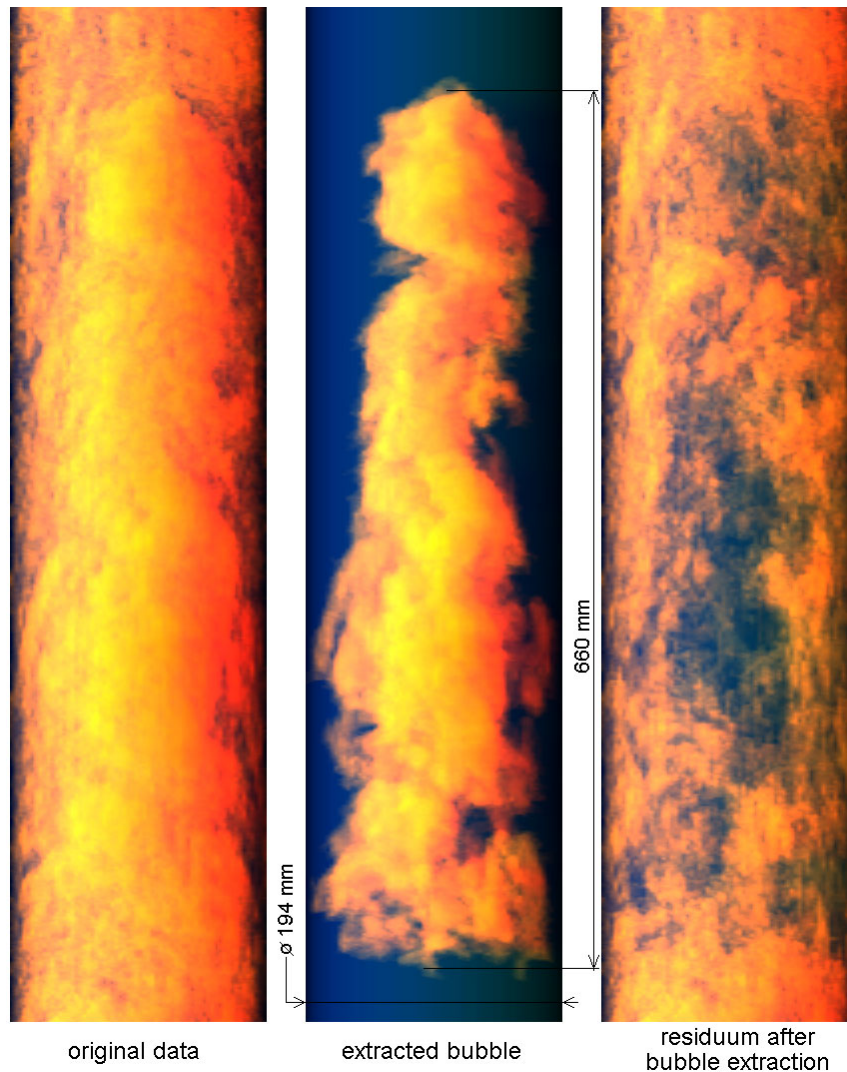


Fig. 7: Example of the extraction of a large bubble from the signal of the wire-mesh sensor (superficial velocities: $J_{\text{air}} = 1.3 \text{ m/s}$ and $J_{\text{water}} = 1 \text{ m/s}$)

5. Conclusions

Detailed quantitative information about bubble size distributions of a gas-liquid flow in a pipe of DN200 and an advanced visualization of the flow structure are presented for the first time. The results were obtained by a wire-mesh sensor with a measuring matrix of 64x64 points, which delivers 2500 frames per second. They were compared to earlier measurements at a pipe of DN50. Similar to the small pipe it was found also in the large pipe that the monomodal bubble size distribution characteristic for low gas flow rates transits to a bimodal distribution when the superficial gas velocity is increased. This transition was observed earlier in the small pipe. The slug flow

resulting in the small pipe was not found in the large pipe. In this sense, the measurements confirm the findings of Ohnuki [8], though the appearance of the bimodal bubble size distribution points at a certain similarity of the processes.

References

- [1] A. Schaffrath, A.-K. Krüssenberg, F.-P. Weiss, E. F. Hicken, M. Beyer, H. Carl, J. Schuster, P. Schuetz, M. Tamme, 2001, TOPFLOW - a new multipurpose thermohydraulic test facility for the investigation of steady state and transient two-phase flow phenomena, *Kerntechnik*, **66**(2001)4, pp. 209-212.
- [2] A. Schaffrath, A.-K. Krüssenberg, F.-P. Weiss, H.-M. Prasser, 2002, Die Mehrzweck-Thermohydraulikversuchsanlage TOPFLOW des Forschungszentrums Rossendorf e.V. - Aufbau, Ziele und Perspektiven, *Atomwirtschaft - Atomtechnik*, **47**(2002)6, pp. 383-388.
- [3] A. Schaffrath, E. F. Hicken, H. Jaegers, H.-M. Prasser, 1999, Operation conditions of the emergency condenser of the SWR1000, *Nuclear Engineering and Design*, **188**(1999) pp. 303-318.
- [4] H.-M. Prasser, A. Böttger, J. Zschau, 1998, A new electrode-mesh tomograph for gas-liquid flows *Flow Measurement and Instrumentation*, **9** (1998), 111-119.
- [5] H.-M. Prasser, M. Beyer, A. Böttger, H. Carl, D. Lucas, A. Schaffrath, P. Schütz, F.-P. Weiss, J. Zschau, Influence of the pipe diameter on the structure of the gas-liquid interface in a vertical two-phase pipe flow, NURETH-10, Seoul, October 5-9, 2003, paper A00308, submitted.
- [6] H.-M. Prasser, D. Scholz, C. Zippe, 2001, Bubble size measurement using wire-mesh sensors, *Flow Measurement and Instrumentation*, 12/4, pp.299-312, 2001.
- [7] H.-M. Prasser, E. Krepper, D. Lucas, 2002, Evolution of the two-phase flow in a vertical tube - decomposition of gas fraction profiles according to bubble size classes using wire-mesh sensors, *International Journal of Thermal Sciences*, **41** (2002) 17-28.
- [8] A. Ohnuki, H. Akimoto, 2000, Experimental study on transition of flow pattern and phase distribution in upward air-water two-phase flow along a large vertical pipe, *International Journal of Multiphase Flow*, **26**(2000)367-386.
- [9] W. H. Leung, C. S. Eberle, Q. Wu, T. Ueno, M. Ishii, 1995, Quantitative characterization of phasic structure developments by local measurement methods in two-phase flow. In: *Proc. of the Second Int. Conf. on Multiphase Flow*, 1995, Kyoto, IN2-17-IN2-25.
- [10] T. J. Liu, S. G. Bankoff, 1993, Structure of air-water bubbly flow in a vertical pipe - II. Void fraction, bubble velocity and bubble size distribution. *Int. J. Heat Mass Transfer*, **36**(4), pp. 1061 - 1072.
- [11] A. Serizawa, I. Kataoka, 1988, Phase distribution in two-phase flow. In: N. H. Afgan (Ed.), *Transient Phenomena in Multiphase Flow*. Hemisphere, 1988, New York. pp. 179-224.
- [12] A.-K. Krüssenberg, H.-M. Prasser, A. Schaffrath, 2000, A new criterion for bubble slug transition in vertical tubes, *Kerntechnik*, **65/1**(2000), pp. 7-13.

Acknowledgement

The work is carried out in the frame of a current research project funded by the German Federal Ministry of Economics and Labour, project number 150 1265. Electronic equipment for wire-mesh sensors was developed in a close co-operation with TELETRONIC GmbH in Rossendorf (www.tz-rotech.de/teletronic/). The authors express their gratitude to the team of developers of TELETRONIC, in persona: D. Peters, G. Pietzsch, W. Taubert and M. Trepte.